Journal of Peptide Science
J. Peptide Sci. **4**: 101–110 (1998)

Solution Conformation of an Immunogenic Peptide from HRV2: Comparison with the Conformation Found in a Complex With a Fab Fragment of an anti-HRV2 Neutralizing Antibody

M. ANTÒNIA MOLINS[1]*, MIQUEL ÀNGEL CONTRERAS[1], IGNACIO FITA[2] and MIQUEL PONS[1]

[1] Departament de Química Orgànica, Universitat de Barcelona, Barcelona, Spain
[2] Centre d'Investigació i Desenvolupament, Consejo Superior de Investigaciones Científicas, Barcelona, Spain

Received 6 May 1997
Accepted 26 May 1997

Abstract: The conformation of a [15]-peptide (H-VKAETRLNPDLQPTE-NH_2) from VP2 of rhinovirus HRV2 complexed with a Fab fragment was previously shown by X-ray crystallographic studies to be similar to the one found in the corresponding region of HRV1A. Antibodies raised against this peptide bind to and neutralize HRV2. In order to identify structural features preserved in solution that may explain the ability of this short peptide to mimic the structure of the protein surface, the peptide has been studied by NMR in aqueous solution as well as under denaturing conditions.

The peptide is shown to be a random coil in solution. However, the sequence forming a 3_{10} helix in the complex is biased into a helical conformation according to NOE intensity data as well as from urea and pH titrations. This sequence adopts the same conformation in an unrelated protein. NOE data suggest that a β-turn found in the complex may be sampled in solution. Also, Glu4, interacting with Arg6 in the crystal, has a reduced pK_a value in solution. It is concluded that the local structure present in the random coil state of VP2(156–170) contains enough information to direct the production of antibodies that bind to and neutralize HRV2.

Keywords: NMR; random coil; rhinovirus; synthetic vaccine

INTRODUCTION

Immunization with synthetic peptides has given rise to neutralizing antibodies for several viral diseases such as influenza [1], the common cold [2], foot-and-mouth disease [3] and AIDS [4, 5], as well as bacterial and parasitic diseases [6, 7]. These examples suggest that, in spite of the expected high flexibility of short peptides, they may contain enough structural information to direct the recognition of the cognate region in an intact protein on the surface of the pathogen.

Abbreviations: ES-MS, electron spray mass spectrometry; HRV, human rhinovirus; MALDI-TOF-MS, matrix-assisted laser desorption and ionization-time of flight mass spectrometry; PDB, Protein Data Bank; TOCSY, total correlation spectroscopy; VP, Viral capsid protein.

* Present address: Unitat de RMN, Serveis Científico-Tècnics, Universitat de Barcelona.
Address for correspondence: Miquel Pons, Departament de Química Orgànica, Universitat de Barcelona, Martí Franquès, 1–11, E-08028, Barcelona, Spain

CCC 1075-2617/98/020101-10

Human rhinoviruses (HRVs) are the main causal agent of the common cold and belong to the picornavirus family. The capsid is composed of 60 copies of each of four proteins VP1, VP2, VP3 and VP4, arranged on an icosahedral surface [8]. Proteins VP1–VP3 contain an eight-stranded β-barrel. The secondary structural elements of this barrel are connected by hypervariable loops where binding sites for neutralizing antibodies are generally located. Three neutralizing antigenic sites, designated A, B and C, have been defined for HRV2 by analysis of escape mutants [9] and by using structural information available for a closely related serotype, HRV1A [10].

Recently, the three-dimensional structure of the complex between the Fab fragment of an anti-human rhinovirus neutralizing antibody (8F5) and a cross-reactive peptide (VP2(156–170)) from HRV2 has been determined [11]. This peptide, with the sequence H-VKAETRLNPDLQPTE-NH_2, corresponds to residues 156–170 of the viral capsid protein VP2 and is located at site B. This peptide includes the minimal binding site of 8F5 (TRLNPD) [12] as well as those residues whose mutations give rise to escape neutralization by this antibody [9, 11]. The structure of the peptide antigen is well defined in the refined crystal structure of the complex at 2.1 Å resolution (J. Tormo and I. Fita, unpublished results. The published structure is at 2.5 Å resolution) and is shown to adopt a similar conformation to the one found in the corresponding region in HRV1A [10]. Furthermore, VP2(156–170) has been used to raise peptide-specific antisera which both bind to and neutralize HRV2 [2, 12]. These observations suggest that the structure found in the antibody complex reflects the conformation that VP2(156–170) adopts in the intact protein and that this conformational preference is encoded in the sequence of the isolated peptide.

In order to test this hypothesis we have studied the conformation of VP2(156–170) in solution using NMR. According to a number of different criteria [13], the peptide is a random coil in solution. However, different experimental evidences indicate that a particular region shows a biased sampling of the Ramachandran map that may facilitate folding in the conformation found by X-ray. This hypothesis is supported by the similar folding observed for the same sequence in a completely unrelated protein.

These observations highlight the importance of the 'unfolded' state in determining the folding properties of a peptide and suggest that local interactions present in the coiled-coil may contain enough information to direct the formation of antibodies capable of binding to and neutralizing the intact virus.

MATERIALS AND METHODS

Peptide VP2(156–170), H-VKAETRLNPDLQPTE-NH_2, was synthesized by solid-phase methodology using the Boc–benzyl strategy. After cleavage and deprotection with anhydrous HF, the crude material was purified by medium pressure chromatography. The resulting peptide had correct amino acid analysis and mass-spectra (MALDI-TOF and EI-MS) and its purity was estimated to be higher than 98% by HPLC and capillary electrophoresis. NMR samples typically had concentrations of between 2 and 5 mM. Aggregation was ruled out by recording a series of spectra at different concentrations, down to 0.082 mM. Samples in urea were prepared in buffer (15 mM Na-phosphate, pH = 5.18) with freshly dissolved urea (Aldrich).

NMR spectra were recorded at 500 MHz in a Varian VXR-500 or Bruker Avance DMX-500 instruments. Typical 2D experiments were obtained with a spectral width of 5000 Hz in both dimensions using 2048×256 complex data points zero-filled to 4096×1024 points. Spectra were processed using a Gaussian function or a shifted sine-bell and forward linear prediction in $f1$ to double the time domain. Water was eliminated either by presaturation using the transmitter or by placing a Watergate modulus prior to data acquisition. Mixing times in TOCSY spectra were 60–80 ms. NOESY spectra were recorded at least at four mixing times in the range 50–400 ms. ROESY mixing times were in the range 50–200 ms. A 2D NOESY-TOCSY experiment was carried out at 25 °C in a 3.7 mM sample at pH 5.22 in H_2O/D_2O 9 : 1 using mixing times of 150 ms (NOESY) and 70 ms (TOCSY).

Temperature coefficients were measured in the range 2–35 °C (2 °C increments) for samples in water and from 10 to 20 °C (3 °C increments) for samples in water–DMSO mixtures.

Titrations were carried out at 25 °C in an unbuffered peptide sample by recording a series of 29 TOCSY spectra at *ca.* 0.15 pH unit intervals from pH = 1.90 to pH = 6.87. pH-dependent chemical shifts were fitted to the equation for a one-step titration:

$$\delta_{obs} = \delta_{HA} + (\delta_A - \delta_{AH}) \frac{1}{1 + 10^{pK - pH}}$$

RESULTS AND DISCUSSION

Conformation of Complexed VP2(156–170)

The structure of VP2(156–170) complexed with 8F5 determined by X-ray by Tormo *et al.* [11] has a compact folded conformation with Lys2 and Gln12 Cα atoms only 6.9 Å apart (Figure 1). In the N-terminal half of the peptide, two turns are observed: a γ-turn involving residues Ala3-Thr5 and a type I β-turn between residues Ala3 and Arg6. A salt bridge between Glu4 and Arg6 participates in the stabilization of the conformation in this part of the molecule. The C-terminal half of the molecule presents a short 3_{10}-helix, initiated at Pro9 and stabilized by Asn8 acting as an N-cap by forming a hydrogen bond between its side-chain carbonyl and the backbone NH of Asp10. The Gln12 side chain seems to be playing a central role in the organization of this structure as it interacts with Asn8, probably stabilizing the 3_{10}-helix, but also forming two hydrogen bonds with the main chain atoms of Glu4.

Both the β-turn and the 3_{10}-helix overlap partially with the minimal binding site (TRLNPD) and are the target of mutations that allow viruses to escape neutralization. Two of them (Glu159Gly and Arg161Thr) affect the β-turn region while the other three (Asn163Tyr, Asn163Ser and Pro164Ser) would disrupt the initiation of the 3_{10} helix.

The Sequence NPDXQP Forms a Similar 3_{10}-Helix in Urease

The sequence of the hexapeptide NPDLQP that forms a 3_{10}-helix in the peptide–Fab complex, was searched for in the Swiss-prot database. The probability of random occurrence of this particular hexapeptide in release 33 of Swiss-prot (18,531,384 amino acids) is 0.33. A complete match of the hexapeptide was found in the iron-regulated outer membrane virulence protein precursor of *Vibrio cholerae* (entry P04936). Unfortunately, the 3D structure of this protein is not present in the Protein Data Bank. However, a very similar sequence Asn-Pro-Asp-X-Gln-Pro (X = Val, Met, Ile) is found in the alpha subunit of urease (EC 3.5.1.5) from different species and that of *Klebsiella aerogenes* is found in the PDB (1 KAU and related entries [14]).

Examination of the conformation of the two segments showed that they are indeed similar except that the C-terminal proline was traced on the *cis*-conformation in VP2(156–170) complexed with the Fab but is *trans* in urease. This residue was therefore excluded from the calculation of the root mean square difference (RMSD) of the Cα carbons after superimposition. Instead, the comparison was extended to the previous residue in the sequence. The RMSD of residues 7–12 of VP2(156–170) with residues 100–105 of urease is 0.96 Å and the side chains retain the same orientation (Figure 2). A comparison of the two X-ray structures reveals similar interactions in both segments: the side chain of Asn is involved in an N-cap interaction with the amide proton of Asp. At the same time, the side chain of Gln is folded back to make contacts with either Asp or Pro at the beginning of the helix. The proline residue at the beginning of the sequence is also likely to participate in the stabilization of the helix as it can adopt the correct dihedral angles and, by restricting the conformational freedom of the

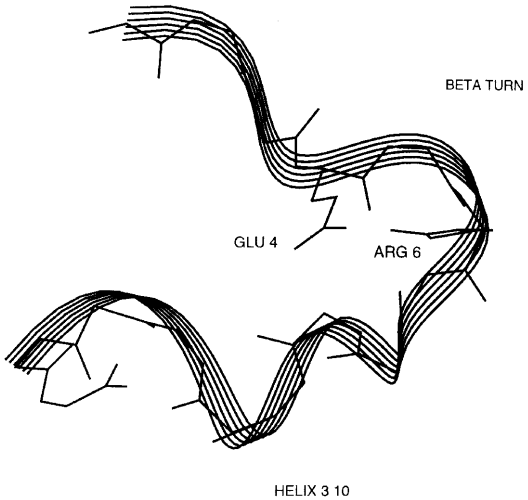

Figure 1 Structure of H-VKAETRLNPDLQPTE-NH_2 peptide complexed with 8F5 Fab. Only the side chains of Glu4 and Arg6 are displayed.

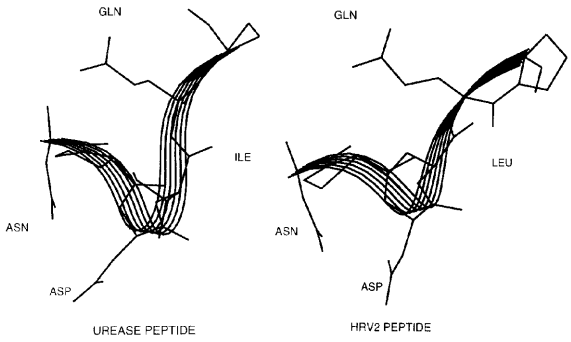

Figure 2 Detail of the 3D structure of the NPDLQP region of H-VKAETRLNPDLQPTE-NH_2 complexed with 8F5-Fab and residues 100–106 (NPDIQP) of the α-subunit of *Klebsiella aerogenes* urease. Both structures have been oriented to minimize the RMSD between the positions of equivalent Cα atoms and then displaced for clarity.

preceding residue, could reduce the conformational penalty associated with formation of the N-cap interaction.

The similarity of the structure of the hexapeptide in completely unrelated proteins confirms an intrinsic structural propensity for this segment to fold in the conformation found in the Fab complex.

Table 1 Proton Chemical Shifts (Relative to Dioxane) of VP2(156–170) Peptide at 275 K, pH = 3.17

Residue	NH	αH	βH		Others
Val1	–	3.78	2.20	γCH_3	1.02
Lys2	8.87	4.34	1.79	γCH_2	1.46
				δCH_2	1.69
				εCH_2	2.99
				εNH_{3+}	7.65
Ala3	8.80	4.29	1.39		
Glu4	8.73	4.42	2.10/1.98	γCH_2	2.48
Thr5	8.54	4.29	4.15	γCH_3	1.20
Arg6	8.68	4.35	1.83/1.77	γCH_2	1.62
				δCH_2	3.20
				NH	7.28
Leu7	8.60	4.33	1.61	γH	1.52
				δCH_3	0.92/0.85
Asn8	8.76	4.94	2.89/2.74	γNH_2	7.88/7.18
Pro9	–	4.39	2.29	γCH_2	2.16
				δCH_2	3.79
Asp10	8.59	4.66	2.93/2.80		
Leu11	8.22	4.35	1.67	γH	1.60
				δCH_3	0.95/0.87
Gln12	8.42	4.62	2.12/1.96	γCH_2	2.41
				δNH_2	7.70/7.05
Pro13	–	4.51	2.34	γCH_2	2.04/1.94
				δCH_2	3.78/3.68
Thr14	8.56	4.29	4.21	γCH_3	1.24
Glu15	8.61	4.39	2.15/1.99	γCH_2	2.48
				NH_2	7.83/7.31

VP2(156–170) is a Random Coil in Solution

TOCSY and NOESY or ROESY spectra of the peptide were recorded in aqueous solution (H_2O/D_2O 9 : 1) under the following conditions: (1) pH = 5.22, 25 °C; (2) pH = 5.22, 2 °C; (3) pH = 3.17, 25 °C; (4) pH = 3.17, 2 °C; (5) pH = 5.18, 8 M urea, 15 mM sodium phosphate, 25 °C; (6) pH = 5.18, 8 M urea, 15 mM sodium phosphate, 2 °C. The peptide was also studied in H_2O–DMSO ($\chi H_2O = 0.91$) under two different sets of conditions: (7) pH = 3.79, 25 °C; (8) pH = 3.76, 10 °C. Complete sequential assignment could be obtained in all the above-mentioned conditions. Representative chemical shifts are reported in Tables 1–3.

Chemical shifts of CH_α protons are within 0.05 p.p.m. of the random coil values measured in 8 M urea. Temperature coefficients were measured in water (pH = 3.3) and water–DMSO (pH = 3.4) solutions (Table 4). The large negative values for all amide protons (-5.1 to -9.1) indicate they are exposed to solvent in both conditions. All $J_{NHCH\alpha}$ have average values between 6 and 7 Hz.

NOESY spectra in water at pH = 5.22 at 25 and 2 °C with a mixing time of 100 ms show, in addition to typical fingerprint signals, a set of $d_{NN}(i,i+1)$ cross peaks between residues 4–5, 5–6, 7–8, 10–11 and 11–12 (Figure 3). The $d_{NN}(i,i+1)$ cross peak between 6–7 is very close to the diagonal and could only be detected unequivocally at 25 °C with a mixing time of 150 ms. At pH 3.17, 2 °C and with a mixing time of 100 ms, only the 5–6, 10–11 and 11–12 cross peaks could be detected. At longer mixing times 4–5 and 7–8 were also observed.

Although in aqueous solutions $d_{NN}(i,i+1)$ cross peaks are more intense at lower temperatures, no improvement was observed in H_2O–DMSO at 10 °C (results not shown). In 8 M urea (pH = 5.18, 2 °C)

Table 2 Proton Chemical Shifts (Relative to Dioxane) of Backbone NH in Different Conditions of Temperature, pH and Solvent

Conditions	Val[1]	Lys[2]	Ala[3]	Glu[4]	Thr[5]	Arg[6]	Leu[7]	Asn[8]	Pro[9]	Asp[10]	Leu[11]	Gln[12]	Pro[13]	Thr[14]	Glu[15]
H_2O, pH = 3.17, T = 2 °C	–	8.87	8.80	8.73	8.53	8.68	8.60	8.76	–	8.59	8.22	8.43	–	8.56	8.61
H_2O, pH = 3.17, T = 25 °C	–	8.68	8.53	8.49	8.26	8.42	8.33	8.49	–	8.41	8.00	8.22	–	8.27	8.34
H_2O, pH = 5.22, T = 2 °C	–		8.80	8.75	8.55	8.69	8.60	8.72	–	8.42	8.09	8.49	–	8.55	8.61
H_2O, pH = 5.22, T = 25 °C	–		8.56	8.55	8.28	8.44	8.34	8.47	–	8.27	7.92	8.28	–	8.28	>8.38
8 M urea, pH = 5.18, T = 2 °C	–	8.96	8.81	8.78	8.57	8.78	8.67	8.96	–	8.54	8.18	8.63	–	8.54	8.62
8 M urea, pH = 5.18, T = 25 °C	–	8.78	8.57	8.58	8.31	8.52	8.42	8.68	–	8.36	7.97	8.39	–	8.29	8.40
H_2O/DMSO[a], pH = 5.0, T = −10 °C	–	8.85	8.75	8.73	8.41	8.65	8.51	8.65	–	8.40	8.05	8.37	–	8.43	8.53
H_2O/DMSO, pH = 5.0, T = 25 °C	–	8.69	8.54	8.56	8.19	8.40	8.29	8.40	–	8.27	7.89	8.19	–	8.20	8.33

[a] $\chi H_2O = 0.91$.

Table 3 Proton Chemical Shifts (Relative to Dioxane) Corresponding to CH_α in Different Conditions of Temperature, pH and Solvent

Conditions	Val[1]	Lys[2]	Ala[3]	Glu[4]	Thr[5]	Arg[6]	Leu[7]	Asn[8]	Pro[9]	Asp[10]	Leu[11]	Gln[12]	Pro[13]	Thr[14]	Glu[15]
H_2O, pH 3.17, $T=2$ °C	3.80	4.34	4.29	4.42	4.29	4.35	4.33	4.94	4.38	4.66	4.36	4.62	4.50	4.29	4.39
H_2O, pH 3.17, $T=25$ °C	3.83	4.35	4.32	4.42	4.31	4.36	4.33	4.94	4.39	4.66	4.35	4.62	4.50	4.31	4.39
H_2O, pH = 5.22, $T=2$ °C	3.80		4.32	4.34	4.30	4.35	4.32	4.95	4.38	4.56	4.34	4.61	4.51	4.30	4.30
H_2O, pH = 5.22, $T=25$ °C			4.34	4.37	4.32	4.37	4.33	4.97	4.39	4.57	4.35	4.62	4.52	4.32	4.32
8 M urea, pH = 5.18, $T=2$ °C	3.80	4.37	4.33	4.38	4.32	4.40	4.33	4.96	4.42	4.62	4.38	4.60	4.53	4.32	4.35
8 M, urea, pH = 5.18, $T=25$ °C	3.83	4.40	4.37	4.40	4.36	4.41	4.35	4.97	4.41	4.62	4.39	4.62	4.53	4.36	4.37
H_2O/DMSO[a], $T=-10$ °C	3.76	4.34	4.30	4.34	4.30	4.34	4.30			4.53	4.32	4.57	4.47	4.28	4.30
H_2O/DMSO, $T=25$ °C	3.79	4.36	4.35	4.37	4.32	4.37	4.35	4.94		4.54	4.35	4.59	4.44	4.29	4.33

[a] $\chi H_2O = 0.91$, pH = 5.0.

Table 4 Temperature Coefficients (in p.p.b./K) for Backbone Amide Protons

Residue	Temp. coeff.	Residue	Temp. coeff.
Lys[2]	−6.5[a] (−5.2[b])	Asn[8]	−8.5 (ND)
Ala[3]	−8.7 (−7.2)	Asp[10]	−6.0 (−6.0)
Glu[4]	−7.8 (−7.8)	Leu[11]	−6.7 (−5.9)
Thr[5]	−8.2 (−7.0)	Gln[12]	−6.8 (−5.5)
Arg[6]	−8.0 (−6.9)	Thr[14]	−9.1 (−7.8)
Leu[7]	−8.5 (−6.8)	Glu[15]	−8.0 (−6.8)

[a] In H_2O/D_2O at pH = 3.3.
[b] In DMSO/H_2O $\chi H_2O = 0.91$ at pH = 3.4.

$d_{NN}(i,i+1)$ cross peaks 4–5, 5–6, 7–8, 10–11 and 11–12 can still be observed in NOESY spectra with mixing times of 100 or 150 ms (Figure 3). A series of consecutive $d_{NN}(i,i+1)$ cross peaks alone do not provide evidence for helical structure. In a recent study of cold, denatured Barstar sequential $d_{NN}(i,i+1)$ NOEs were observed for almost all residues [15]. No $(i,i+3)$ peaks could be detected under any of the conditions studied. A strong sequential cross peak could obscure the expected (on the basis of the X-ray structure) $d_{\alpha N}(9,12)$. However the absence of $(i,i+3)$ peaks was confirmed in a NOESY-TOCSY experiment. From the three consecutive $d_{\alpha N}(i,i+2)$ connectivities predicted by the structure found in the complex only that between Asn8 and Asp10 was visible.

Both Prolines are *trans* in Solution

The two prolines in the sequence could lead to species with *cis*-peptide bonds. In particular, Pro13 was found to be *cis*- in the Fab-complex of the same peptide. No clear evidence for two conformations in slow exchange is present in the NMR spectra. Furthermore, diagnostic $d_{\alpha\delta}(i,i+1)$ NOEs indicate that both prolines are *trans* in the species observed in solution.

NOE Intensity Ratios

Sequential NOEs provide characteristic information on the backbone conformation in (ϕ, ψ) space. The intensity ratio between intramolecular ($d_{\alpha N}(i+1, i+1)$) and sequential ($d_{\alpha N}(i,i+1)$) NOEs ($\sigma_{N\alpha}/\sigma_{\alpha N}$) has been suggested as a measure of the relative population of the α and β regions of the Ramachandran map [15–17]. A value of $\sigma_{N\alpha}/\sigma_{\alpha N}$ of 0.24 [17] is predicted for an extended chain and values of 0.28 ± 0.09 have been described for an unstructured region of denatured barnstar [15]. Spectral overlap only allowed the measurement of $\sigma_{N\alpha}/\sigma_{\alpha N}$ ratios for residues 9 (0.41), 10 (0.43) and 11 (0.18) in VP2(156–170). These values suggest that the first two residues preferentially sample the α region. The ratio between sequential NOEs ($\sigma_{NN}/\sigma_{\alpha N}$) connecting residues 10 and 11 is 0.41, well above the expected value for an extended conformation (0.02) and higher than the values found for unstructured thermolysin peptides [16]. In 8 M urea, the $\sigma_{N\alpha}/\sigma_{\alpha N}$ and $\sigma_{NN}/\sigma_{\alpha N}$ ratios for Asp10, the only ones that could be accurately measured, present slightly lower values of 0.38 and 0.30 but still suggest preferential population of the α region.

Urea-induced Amide Shifts

Urea-induced backbone amide proton chemical shifts can be useful in identifying local structures present even in random coil peptides. In random coil

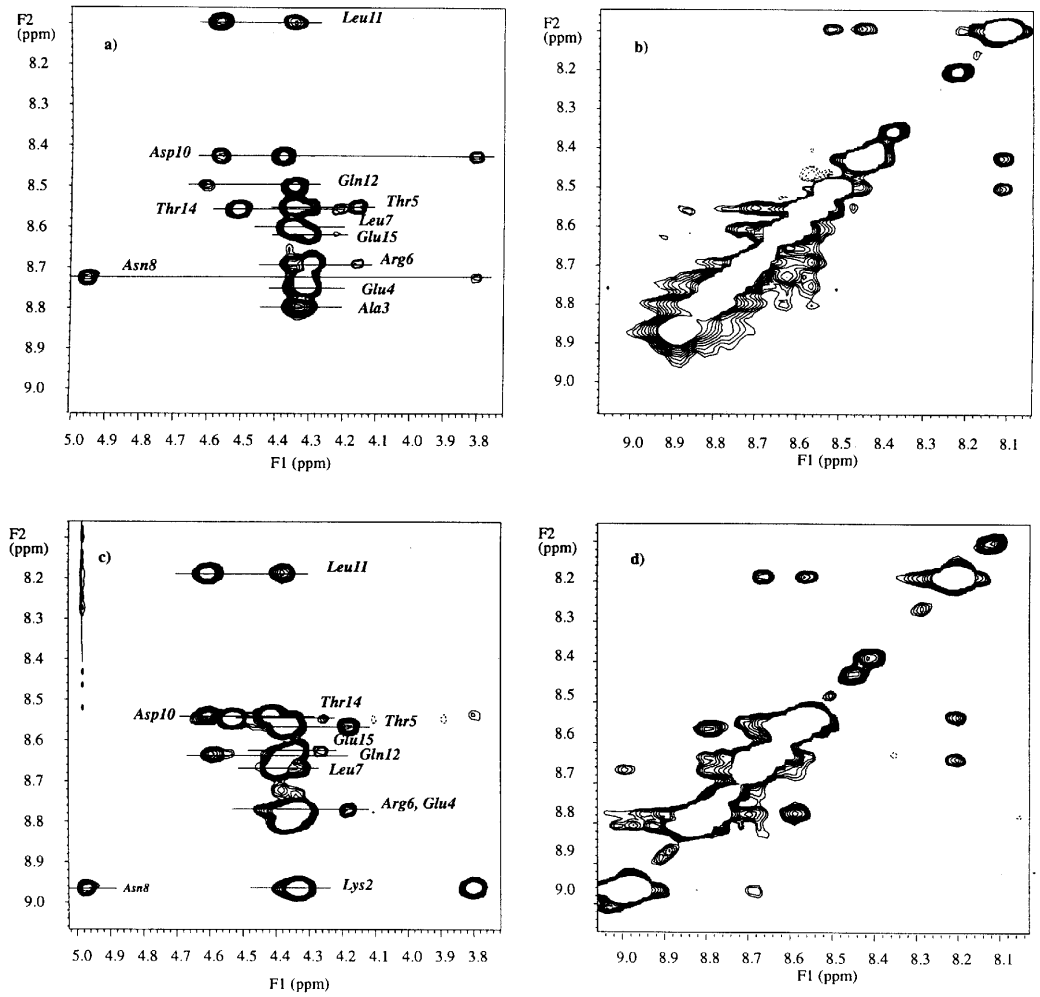

Figure 3 Representative expansions of the CHα–NH (a, c) and NH–NH regions (b, d) of NOESY spectra of H-VKAETRLNPDLQPTE-NH_2 (100 ms mixing time) in 10% D_2O, pH = 5.22 and 2 °C (a, b) and in 8 M urea, 15 mM sodium phosphate, 10% D_2O, pH = 5.18 and 2 °C (c, d). Spectra were acquired under identical conditions and are plotted at the same vertical scale to provide an indication of the relative intensities of the cross peaks.

peptides small downfield shifts (0.03 p.p.m. on average) are observed and the effect seems to be nearly sequence-independent [18] although the residue following Arg in these model peptides showed the largest shift (0.13 p.p.m.). The same trend was also observed in the residues located around two non-consecutive Arg residues in the C-terminal tail of LIMP II, a random coil peptide apparently responsible for targetting lysosomes (M. A. Jimenez, personal communication; [19]). This 'Arg effect' may be rationalized on the basis of the structural complementarity between urea and the guanidinium group that could interfere with side-chain backbone interactions present in the absence of urea. On the other hand, no specific effect could be observed for Asn, Gln or Asp. A plot of the chemical shift of backbone amide protons of VP2(156–170) in water minus those measured in 8 M urea ($-\Delta_{urea}$) is shown in Figure 4. Significant chemical shift differences were observed for residues 6–12, and particularly in the region 8–12. Although isolated shifts around 0.10 p.p.m. are occasionally found in random coil peptides, a cluster of six residues with large shifts suggests some residual structure being disturbed by urea. These residues, with the exception of Leu11, have polar side chains that could be involved in side-chain–backbone interactions that stabilize helical states. Residues with significant urea amide shifts include all of those adopting a 3_{10}-helix in the Fab complex. Additionally, Arg6 could also contribute to the observed shifts in positions 6, 7 and perhaps 8.

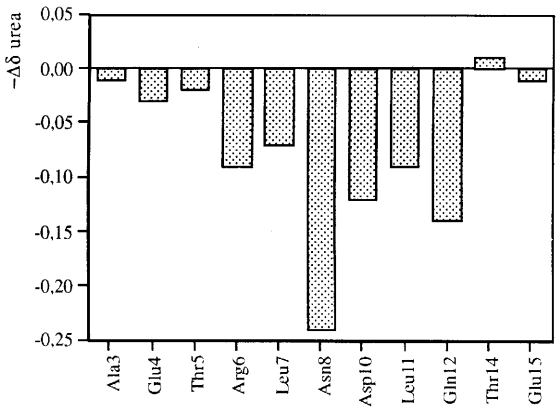

Figure 4 Chemical shifts differences between backbone NH protons in water (pH = 5.22, 2 °C) and in 8 M urea (pH = 5.18, 2 °C, 15 mM sodium phosphate).

pH Titration

Backbone amide proton titration shifts are a very sensitive manifestation of intramolecular hydrogen bonding between carboxylate groups and backbone amide protons [20]. In addition, pK_a perturbations of carboxylate groups and a titration-induced shift in positively charged side chains could indicate the preservation of the salt bridge observed in the complex. Apparent pK_a values of ionizable groups were determined from a series of 29 TOCSY spectra. This procedure allowed the unequivocal determination of the pK_a values of residues with overlapping signals in the 1D spectra like those from the two glutamic acid residues. Chemical shifts, from cross-peak positions, were fitted to the equation for a one-step titration (Figure 5). Protons whose chemical shifts change by more than 50 p.p.b. and with a good fit to the equation for a single ionization process ($R^2 > 0.98$) are shown in Table 5. The measured pK_a

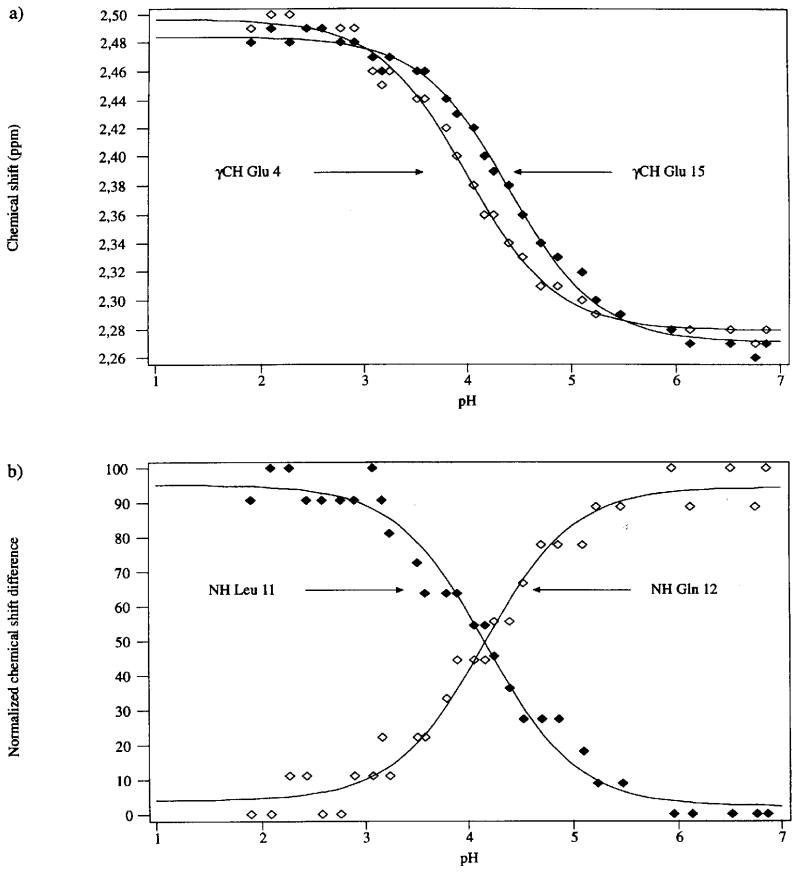

Figure 5 Plots of pH titrations of (a) CH_γ chemical shifts of Glu4 and Glu15 and (b) normalized chemical shifts differences of backbone NH protons of Leu11 and Gln12. Normalization was performed by subtracting the lowest value found in the titration (that is the one measured at high pH for Gln12 and at low pH for Leu11) from chemical shifts measured at each pH, and dividing by the chemical shift difference between both ends of the titration.

Table 5 Apparent pK_a Values of pH-sensitive Protons of VP2(156–190)

Residue	Nuclei	pK_a (experimental)	pK_a (intrinsic)	$(\delta_{HA}-\delta_A)$ $\times 10^3$ p.p.m.
Glu[4]	NH	3.87 ± 0.06	4.2 ± 0.1	− 75
	CHγ	3.98 ± 0.03		218
Asp10	NH	3.95 ± 0.03	3.9 ± 0.1	165
	CHβ1	3.89 ± 0.03		247
	CHβ2	3.96 ± 0.03		261
Leu11	NH	4.17 ± 0.05	–	103
Gln12	NH	4.15 ± 0.06	–	− 81
Glu15	NH	4.35 ± 0.06	4.2 ± 0.1	− 64
	CHγ	4.39 ± 0.03		213

for Asp10 (3.93) and Glu15 (4.37) correspond to the expected intrinsic values in the absence of significant effects from other charged sites in the peptide [21] while that of Glu4 (3.92) is around 0.3 pK_a units lower, indicating an effect from a nearby charged group. There are two charged residues (Lys2 and Arg6) one on either side of Glu4 that could be responsible for the observed pK_a shift. However, no pH-dependent chemical shifts could be detected in either Lys or Arg side-chain protons, indicating that the salt bridge observed in the Fab complex is not maintained in the free peptide in solution.

Apart from the ionizable residues, significant shifts were only observed for the NH protons of Leu11 and Gln12 during the pH titration. Both groups shift in opposite directions but the middle points of the titration coincide (Figure 5(b)). Protonation of an Asp side chain is known to cause intrinsic downfield shifts in its own amide proton and in that of the following residue. On the other hand, protonation of a γ-carboxyl group of Glu induces upfield shifts in amide protons to which the Glu side chain can form hydrogen bonds [20]. The upfield shift observed for the NH of Gln12 (− 81 p.p.b.) is larger than the one observed for Thr14 (− 23 p.p.b.), Glu15 (− 64 p.p.b.), Ala3 (− 25 p.p.b.) or Glu4 (− 75 p.p.b.). This indicates that the NH amide proton of Gln12 forms a hydrogen bond with a carboxylic acid from a side chain. The apparent pK_a is intermediate between that of Asp10 and Glu15 and therefore does not allow an unequivocal assignment of the side chain involved in hydrogen bonding. However, the similarity of the apparent pK_a measured on Leu11 and Gln12 suggests that Asp10, which is most probably responsible for the shift in Leu11, is the one involved in hydrogen bonding to Gln12. These backbone–side chain interactions are favoured if the random coil is populating an α-conformation in this region.

Preservation of the β-turn in Solution?

A conformational feature found in the complex between the viral peptide and 8F5 is a β-turn including residues Ala3–Arg6 stabilized by a salt bridge involving the side chains of Glu4 and Arg6. The involvement of β-turns in peptide–antibody complexes has been found in several X-ray structures of complexes [11, 22, 23] and has also been detected in different antigenic peptides [24–27]. A short helix segment C-terminal to an open turn (with the RGD sequence) has also been found by X-ray in the main antigenic site of foot-and-mouth disease virus [28, 29]. Recent cell recognition studies of FMDV [30] indicate the involvement of residues in the helix for RGD-mediated recognition.

Diagnostic NOEs for a β-turn [27] include a strong $d_{NN}(i,i+1)$ NOE between residues in positions 3 and 4 of the turn (2.2 Å) and a weaker $d_{\alpha N}(i,i+2)$ NOE between positions 2 and 4 (3.6 Å in type I and 3.3 Å in type II). A $d_{\alpha N}(i,i+2)$ cross peak typical of a β-turn was observed between Glu4 and Arg6 at 2 °C and a pH of 3.17 at all mixing times. At pH = 5.22 accidental coincidence of the CH_α protons of Glu4 and Arg6 prevents the observation of this cross peak. Weak $d_{\beta N}(i,i+2)$ between the same residues indicate the close proximity of these two residues at both pH values. The $(i,i+2)$ NOEs and a relatively strong $d_{NN}(i,i+1)$ NOE between Thr5 and Arg6 could be taken as an indication that the β-turn found in the crystal is being sampled in solution. However, the large temperature coefficient of Arg6 (− 8 p.p.b. K^{-1}) suggests that it does not participate in a hydrogen bond and it has been shown that weak $(i,i+2)$ NOEs can also be observed in random coil peptides [13]. Therefore, the question of the preservation of the β-turn of VP2(156–170) in solution remains open.

CONCLUSIONS

Our results show that VP2(156–170) is a random coil in solution defined as the ensemble of conformations adopted by a peptide in the absence of non-local interactions. One can define two intermediate situations between a completely disordered conformation and a well-defined, unique, static structure. Nascent structures have a reduced number of long-range contacts of the type that stabilize well-defined secondary structures. On the other hand what we call a 'biased-coil' state is the result

of non-random population of the standard accessible regions of the Ramachandran map. The absence of long-range interactions differentiate the biased-coil from nascent structures. A biased-coil has a rather high information content which is not obvious from the primary structure alone and can be experimentally characterized (for example, by the relative intensities of local NOEs or by perturbation of the conformational equilibrium using urea or pH changes).

'Random' is associated with 'non-deterministic' which means that one could generate a correct description of the coil state by randomly choosing pairs of dihedral angles from the globally allowed regions of the Ramachandran map. On the other hand, 'biased' suggests preferential sampling of only a subset of the initial possible angles. However, a biased coil is just a special case of random coil since the preferential sampling has a local origin.

The conformation of VP2(156–170) is probably best defined as a biased coil, with a preferential population of the α region of the Ramachandran map, probably through side-chain–backbone interactions, in the region that forms a 3_{10} helix in the complex and, perhaps, a small tendency to populate a β-turn between residues Ala3 and Arg6 as it is found in the Fab complex. Thus, the two structural features observed in the crystal structure of the peptide complexed with a Fab seem to be 'predetermined' in this particular random coil peptide.

Biased conformational sampling in VP2(156–170) facilitates folding into the conformation found in the crystal structure. A correlation between the conformational preferences of random coils and the structure adopted by the same molecule when folded under native conditions has already been observed [13]. Sequences with conformational bias may act as nucleation points for folding since the entropic cost associated with the transition from a highly disordered ensemble to a unique conformation is reduced. Similarly, peptide recognition is associated with an entropic loss and may involve a similar development of the 'latent' structure present in the random coil. This may provide an explanation for the striking fact that a random coil peptide can direct the production of antibodies capable of binding and neutralizing the intact virus as is the case for VP2(156–170) and HRV2.

Acknowledgements

This work has been supported by DGICYT (PB94-0924) and by the Generalitat de Catalunya (Centre de Referència en Biotecnologia). We thank Mr Jordi Bacardit for help in the synthesis of the peptide, Dr D. Blaas who pointed out the interest of structural research on the 8F5 system and Dr M. A. Jimenez for providing unpublished information on urea-induced shifts for a number of peptides. We acknowledge the use of the NMR facilities of the Serveis Científico Tècnics of the Universitat de Barcelona.

REFERENCES

1. G. M. Muller, M. Shapira and R. Arnon (1982). Anti-influenza response achieved by immunization with a synthetic conjugate. *Proc. Natl Acad. Sci. USA 79*, 569–573.
2. M. J. Francis, G. Z. Hastings, D. V. Sangar, R. P. Clark, A. Syred, B. E. Clarke, D. J. Rowlands and F. Brown (1987). A synthetic peptide which elicits neutralizing antibody against human rhinovirus type 2. *J. Gen. Virol. 68*, 2687–2691.
3. N. R. Parry, P. V. Barnet, E. J. Ouldridge, D. J. Rowlands and E. Brown (1989). Neutralizing epitopes of type O foot-and-mouth disease virus II. Mapping three conformational sites with synthetic peptide reagents. *J. Gen. Virol. 70*, 1493–1503.
4. K. Javaherian, A. J. Langlois, G. J. LaRosa, A. T. Profy, D. P. Bolognesi, W. C. Herlihy, S. D. Putney and T. J. Mathews (1990). Broadly neutralizing antibodies elicited by the hypervariable neutralizing determinant of HIV-1. *Science 250*, 1590–1593.
5. J. M. Rini, R. L. Stanfield, E. A. Stura, P. A. Salinas, A. T. Profy and I. A. Wilson (1993). Crystal structure of a human immunodeficiency virus type 1 neutralizing antibody, 50.1, in complex with *his* V3 loop peptide antigen. *Proc. Natl Acad. Sci. USA 90*, 6325–6329.
6. F. Audibert, M. Jolivet, L. Chedid, R. Arnon and M. Sela (1982). Successful immunization with a totally synthetic diphtheria vaccine. *Proc. Natl Acad. Sci. USA 79*, 5042–5046.
7. M. E. Patarroyo, R. Amador, P. Clavijo, A. Moreno, F. Guzman, P. Romero, R. Tascon, A. Franco, L. A. Murillo, G. Ponton and G. Trujillo (1988). A synthetic vaccine protects humans against challenge with asexual blood stages of *Plasmodium falciparum* malaria. *Nature 332*, 158–161.
8. M. G. Rossman and J. E. Johnson (1989). Icosahedral RNA virus structure. *Annu. Rev. Biochem. 58*, 533–573.
9. G. Appleyard, S. M. Russell, B. E. Clarke, S. A. Speller, M. Trowbridge and J. Vadolas (1990). Neutralization epitopes of human rhinovirus type 2. *J. Gen. Virol. 71*, 1275–1282.
10. S. Kim, T. J. Smith, M. S. Chapman, M. G. Rossmann, D. C. Pevear, F. J. Dutko, P. J. Felock, G. D. Diana and M. A. McKinlay (1989). Crystal structure of human rhinovirus serotype 1A (HRV1A). *J. Mol. Biol. 210*, 91–111.

11. J. Tormo, D. Blaas, N. R. Parry, D. Rowlands, D. Stuart and I. Fita (1994). Crystal structure of a human rhinovirus neutralizing antibody complexed with a peptide derived from viral capsid protein VP2. *EMBO J. 13*, 2247–2256.
12. G. Z. Hastings, S. A. Speller and M. J. Francis (1990). Neutralizing antibodies to human rhinovirus produced in laboratory animals and humans that recognize a linear structure from VP2. *J. Gen. Virol. 71*, 3055–3059.
13. L. J. Smith, K. M. Fiebig, H. Schwalbe and C. M. Dobson (1996). The concept of a random coil. Residual structure in peptides and denatured proteins. *Folding Design 1*, R95–R106.
14. E. Jabri, M. H. Lee, P. A. Hausinger and P. A. Karplus (1992). Preliminary crystallographic studies of urease from jack bean and from *Klebsiella aerogenes*. *J. Mol. Biol. 227*, 934–937.
15. K. Wong, S. M. Freund and A. Fersht (1996). Cold denaturation of Barstar: ^{1}H, ^{15}N and ^{13}C NMR assignment and characterization of residual structure. *J. Mol. Biol. 259*, 805–816.
16. M. A. Jimenez, M. Bruix, C. Gonzalez, F. J. Blanco, J. L. Nieto, J. Herranz and M. Rico (1995). CD and ^{1}H-NMR studies on the conformational properties of peptide fragments from the C-terminal domain of thermolysin. *Eur. J. Biochem. 211*, 569–581.
17. J. Saulitis and E. Liepins (1990). Quantitative evaluation of interproton distances in peptides by two-dimensional Overhauser effect spectroscopy. *J. Magn. Reson. 87*, 80–91.
18. M. A. Jimenez, J. L. Nieto, M. Rico, M. Santoro, J. Herranz and F. J. Bermejo (1986). A study of the NH NMR signals of Gly-Gly-X-Ala tetrapeptides in H_2O at low temperature. *J. Mol. Struct. 143*, 435–438.
19. I. V. Sandoval, J. J. Arredondo, J. Alcalde, A. Gonzalez-Noriega, J. Vandekerckhove, M. A. Jimenez and M. Rico (1994). The residue Leu(Ile)^{475}-Ile(Leu,Val,Ala)^{476}, contained in the extended carboxyl cytoplasmic tail, are critical for targeting of the resident lysosomal membrane protein LIMP II to lysosomes. *J. Biol. Chem. 269*, 6622–6631.
20. A. Bundi and K. Wüthrich (1979). Use of amide ^{1}H-NMR titration shifts for studies of polypeptide conformation. *Biopolymers 18*, 299–311.
21. M. Delepierre, C. M. Dobson, M. Karplus, F. M. Poulsen, D. J. States and R. E. Wedin (1987). Electrostatic effects and hydrogen exchange behaviour in proteins. The pH dependence of exchange rates in lysozyme. *J. Mol. Biol. 197*, 111–130.
22. R. L. Stanfield, T. M. Fieser, R. A. Lerner and I. A. Wilson (1990). Crystal structures of an antibody to a peptide and its complex with peptide antigen at 2.8 Å. *Science 248*, 712–719.
23. J. B. Ghiara, E. A. Stura, R. L. Stanfield, A. T. Profy and I. A. Wilson (1994). Crystal structure of the principal neutralization site of HIV-1. *Science 264*, 82–85.
24. A. P. Campbell, C. McInnes, R. S. Hodges and B. D. Sykes (1995). Comparison of NMR solution structures of the receptor binding domains of *Pseudomonas aeruginosa pili* strains PAO, KB7 and PAK: Implications for receptor binding and synthetic vaccine design. *Biochemistry 34*, 16255–16268.
25. H. J. Dyson, K. J. Cross, R. A. Houghten, I. A. Wilson, P. E. Wright and R. A. Lerner (1985). The immunodominant site of a synthetic immunogen has a conformational preference in water for a type-II reverse turn. *Nature 318*, 480–483.
26. M. Blumenstein, G. R. Matsueda, S. Timmons and J. Hawiger (1992). A β-turn is present in the 392–411 segment of the human fibrinogen γ-chain. Effects of structural changes in this segment on affinity to antibody 4A5. *Biochemistry 31*, 10692–10698.
27. A. P. Campbell, B. D. Sykes, E. Norrby, N. Assa-Munt and H. J. Dyson (1996). Solution conformation of an immunogenic peptide derived from the principal neutralizing determinant of the HIV-2 envelope glycoprotein gp125. *Folding Design 1*, 157–165.
28. D. Logan, R. Abu-Ghazaleh, W. Blakemore, S. Curry, T. Jackson, A. King, S. Lea, R. Lewis, J. Newman, N. Parry, D. Rowlands, D. Stuart and E. Fry (1993). Structure of a major immunogenic site on foot-and-mouth disease virus. *Nature 362*, 566–568.
29. N. Verdaguer, M. G. Mateu, D. Andreu, E. Giralt, E. Domingo and I. Fita (1995). Structure of the major antigenic loop of foot-and-mouth disease virus complexed with a neutralizing antibody: Direct involvement of the Arg-Gly-Asp motif in the interaction. *EMBO J. 14*, 1690–1696.
30. M. G. Mateu, M. L. Valero, D. Andreu and E. Domingo (1996). Systematic replacement of amino acid residues within an Arg-Gly-Asp containing loop of foot-and-mouth disease virus and effect on cell recognition. *J. Biol. Chem. 271*, 12814–12819.

